

On the Illumination Invariance of the Level Lines under Directed Light: Application to Change Detection*

Pierre Weiss[†], Alexandre Fournier[‡], Laure Blanc-Féraud[§], and Gilles Aubert[¶]

Abstract. We analyze the illumination invariance of the level lines of an image. We show that if the scene surface has Lambertian reflectance and the light is directed, then a necessary and sufficient condition for the level lines to be illumination invariant is that the three-dimensional scene be developable and that its albedo satisfy some geometrical constraints. We then show that the level lines are “almost” invariant for piecewise developable surfaces. Such surfaces fit most of the urban structures. This allows us to devise a fast and simple algorithm that detects changes between pairs of remotely sensed images of urban areas, independently of the lighting conditions. We show the effectiveness of the algorithm both on synthetic OpenGL scenes and real QuickBird images. The synthetic results illustrate the theory developed in this paper. The two real QuickBird images show that the proposed change detection algorithm is discriminant. For easy scenes it achieves a rate of 85% detected changes for 10% false positives, while it reaches a rate of 75% detected changes for 25% false positives on demanding scenes.

Key words. level lines, topographic map, illumination invariance, contrast equalization, change detection, remote sensing

AMS subject classifications. 65D18, 68U10, 94A08

DOI. 10.1137/09077744X

1. Introduction. Finding illumination invariant features in an image is a recurrent problem in computer vision (see, for instance, [8, 29] and the references therein). There are many important applications that would benefit from such features including recognition, contrast equalization/enhancement, image registration, and change detection.

Perhaps the most frequently used feature is the set of contours [25]. Contours are generally due to discontinuities in the scene elevation or albedo and are illumination invariant in the sense that they appear on an image for most lighting conditions. An alternative feature was recently proposed by Caselles, Coll, and Morel [4]. The authors show that the *level lines* are invariant to *local contrast changes*. We refer the reader to [7] for a more complete description of the level lines and their properties. The set of all level lines (also called the topographic map) has two important advantages over the contours. First, in the discrete

*Received by the editors November 17, 2009; accepted for publication (in revised form) August 24, 2010; published electronically March 31, 2011.

<http://www.siam.org/journals/siims/4-1/77744.html>

[†]Institut de mathématiques de Toulouse, Université Paul Sabatier, 31062 Toulouse Cedex 09, France (pierre.armand.weiss@gmail.com).

[‡]INRIA, Projet ARIANA, INRIA BP 93, 2004 Route des Lucioles, 06902 Sophia-Antipolis, France (Alexandre.Fournier@sophia.inria.fr).

[§]Laboratoire I3S, UMR 6070 CNRS, Projet ARIANA (CNRS/INRIA/UNSA), INRIA BP 93, 2004 Route des Lucioles, 06902 Sophia-Antipolis, France (laure.blanc_feraud@sophia.inria.fr).

[¶]Laboratoire J.A. Dieudonné, UMR 6621 CNRS, University of Nice-Sophia Antipolis, 06108 Nice Cedex 2, France (gaubert@math.unice.fr).

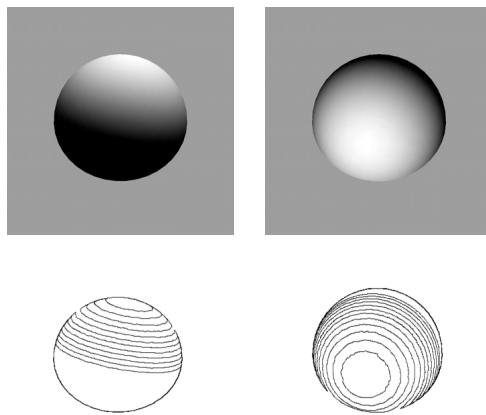


Figure 1. *Top: images of a three-dimensional (3D) dome using a Lambertian model [30] with two different incident light directions. Bottom: some of their level lines.*

setting, the definition of a contour generally depends upon a thresholding parameter, while the topographic map does not. Second, the topographic map allows one to reconstruct an image. Some applications of the topographic maps—such as change detection [28, 1], registration [27], or contrast enhancement [6]—were recently proposed and lead to good results. However, local contrast changes [4] cannot model all *illumination changes* (i.e., variations of the illumination conditions). Figure 1 gives an example of a surface whose level lines are not illumination invariant. Methods that make use of the level lines for their illumination invariance are thus not fully justified.

In this work, we provide necessary and sufficient conditions on the scene geometry for the level lines to be invariant to variations of the incident light direction. In sections 2 and 3, we show that they are invariant only if the scene surface is developable and that its albedo varies in only certain directions of the space. Such surfaces are of little interest as they are not encountered in real scenes. This leads us to analyze the level line invariance for piecewise developable surfaces. We show that the images of such objects have “almost” invariant level lines. While writing this article we discovered a work by Chen, Belhumeur, and Jacobs [8] which shows that the direction of the gradient is “almost” invariant to the light direction of incidence for most scenes. To the best of our knowledge, this result is the closest to our conclusions, as the normal to the level lines is collinear to the gradient. Our attention was also drawn to [16], where the authors use similar tools of differential geometry to derive the image intensity values w.r.t. the surface curvatures and light direction.

In sections 4 and 5, we use the level lines to devise an algorithm adapted to the detection of changes between pairs of registered images. Many manmade structures can be considered piecewise developable. This algorithm is thus particularly adapted to the detection of changes between image pairs of civil infrastructures or high resolution images of urban areas. We focus on the second application. Previous authors had already tried to design change detection algorithms robust to illumination changes. The surveys on change detection by Radke et al. [31] and Lu et al. [24] give some examples of such algorithms. Early attempts include linear contrast equalization [41], local mean and variance normalizations [20], use of the ratio image

[37, 39], or global contrast enhancement [36]. Such approaches share a main weakness: they do not reproduce all of the possible illumination changes. Our experiments using them led to large numbers of false positives. Three works are more closely related to our approach. In [39], the authors make the assumption that the building roofs are flat and have Lambertian reflectance. Under these assumptions, they show that the ratio image can be used to detect shadows and changes independently of the light direction. Their hypotheses on the scene are, however, much more restrictive than ours. In [28], the authors propose an interesting change detection algorithm that makes extensive use of the level lines. However, we will show that their definition of the level lines does not make them illumination invariant features. Reference [1] proposes a method similar to ours. It consists of decomposing the two images into their bilevel lines and comparing them pairwise using geometric features. Its computational complexity is, however, higher.

Finally we compare three different approaches on synthetic images and high resolution QuickBird images. This illustrates the theory developed in sections 2 and 3 and allows us to show the assets and drawbacks of the proposed method on two real test cases. Receiver operating characteristic (ROC) curves show that the proposed algorithm is discriminant and could be used as a component of a more complex statistical change detection framework [23]. Let us point out that there exist many other algorithms based on other invariant features. For instance, [35] uses features such as the Harris corner detector, while [2] evaluates a nonlocal illumination rescaling. These methods are, however, difficult to compare with our approach since they require many decision steps and implicit parameters.

2. Notation, hypotheses, definitions.

2.1. Notation. Let Ω be an open connected set of \mathbb{R}^2 . Let $u : \Omega \rightarrow \mathbb{R}$ be some C^2 function. $\nabla u = [u_1, u_2]$ denotes the gradient of u ; $\nabla^2 u = \begin{bmatrix} u_{11} & u_{12} \\ u_{12} & u_{22} \end{bmatrix}$ denotes its Hessian matrix. Let $q : \mathbb{R}^2 \rightarrow \mathbb{R}^2$, and let $J(q)$ denote the Jacobian of q . Let x and y belong to \mathbb{R}^n . $x \Psi y$ means that x and y are collinear. 0 is collinear to any element of \mathbb{R}^n . Let $\omega \subset \Omega$, and let $\bar{\omega}$ be the closure of ω (w.r.t. the topology induced by the Euclidean metric). $\mathring{\omega}$ and $\text{int}(\omega)$ denote the interior of ω defined as the largest open set contained in ω . $\mu_{\mathbb{R}^n}$ is the Lebesgue measure on \mathbb{R}^n . $\mathcal{M}_{m,n}$ is the space of matrices with m rows and n columns.

The following notation is illustrated in Figure 2. Ω represents the image plane. It is an open connected set of \mathbb{R}^2 . $\mathbf{\Omega}$ represents the object plane, a portion of the plane in \mathbb{R}^3 . $s : \mathbf{\Omega} \rightarrow \mathbb{R}$ designates the scene elevation. $\mathbf{N}(\mathbf{x})$ represents the normal to the scene surface at point $(\mathbf{x}, s(\mathbf{x}))$. $P : (\mathbf{x}, z) \mapsto x$ is a perspective projection on Ω . p is the application defined by

$$(2.1) \quad \begin{aligned} p : \mathbf{\Omega} &\rightarrow \Omega, \\ \mathbf{x} &\mapsto P(\mathbf{x}, s(\mathbf{x})). \end{aligned}$$

We suppose that p is a C^1 diffeomorphism. As a diffeomorphism is bijective, it means physically that the camera can see all points of the surface.

Throughout the article, boldface characters refer to objects that lie in the object plane, while nonboldface characters represent objects in the image plane. For instance $\mathbf{\Omega} = p^{-1}(\Omega)$ represents the object plane. If $x \in \Omega$, we can define $\mathbf{x} = p^{-1}(x)$, which is a point of $\mathbf{\Omega}$.

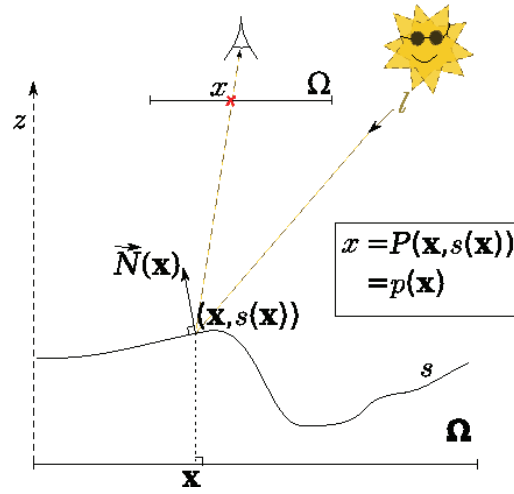


Figure 2. Notation.

Finally, l is a vector in $\mathbb{R}^3 \setminus \{0\}$. $\frac{l}{|l|}$ denotes the light incidence direction, and $|l|$ denotes its intensity.

2.2. Hypotheses on the surface and the light. To model the interactions between a surface and the light, we use the Lambertian model [30, 13]. We make the following hypotheses on the light and the surface.

Hypothesis 1. We suppose that the light is composed of ambient light of amplitude γ (light present uniformly everywhere in the scene) and directed light l (all light rays are parallel with equal intensity).

Hypothesis 2. We suppose that the surface is Lambertian with variable albedo $\alpha : \mathbb{R}^2 \rightarrow \mathbb{R}_*^+$ [13].

Hypothesis 3. To avoid the presence of shadows we suppose that the angle between l and \mathbf{N} is strictly less than $\pi/2$ in a nonempty open set $\mathcal{L} \subset \mathbb{R}^3$. The set of all possible lighting conditions $[l, \gamma]$ is denoted $\mathcal{L} = \mathcal{L} \times \mathbb{R}^+$.

With these hypotheses a scene S is completely described by $S = (s, \alpha)$ and the lighting conditions are completely described by the vector $L = [l, \gamma] \in \mathcal{L}$. Under the Lambertian assumption, the image u of the scene S under lighting conditions L can be written as [30, 13]

$$(2.2) \quad u_{S,L}(x) = (\langle l, \mathbf{N}(\mathbf{x}) \rangle + \gamma) \cdot \alpha(\mathbf{x}),$$

where $\langle \cdot, \cdot \rangle$ stands for the canonical scalar product.

Note. All the results stated later are also valid for the following model of image formation:

$$(2.3) \quad u_{S,L}(x) = \phi((\langle l, \mathbf{N}(\mathbf{x}) \rangle + \gamma) \cdot \alpha(\mathbf{x})),$$

where $\phi : \mathbb{R} \rightarrow \mathbb{R}$ is a strictly monotonic function modeling a global contrast change. To simplify the notation, we make use of only model (2.2).

2.3. Definitions of the level lines. Let $u : \Omega \rightarrow \mathbb{R}$ be some function. We suppose that u is defined everywhere. Throughout this paper the term level line must be understood in the following way.

Definition 1 (level lines). *The level lines of u are the connected components [15] of the isolevels $\{x \in \Omega, u(x) = \lambda\}$.*

This definition is generally used for C^1 functions with nonvanishing gradient. For such functions, the level lines can be shown to be Jordan curves that either are closed or have extremities which lie on the boundary of Ω . For other functions the level lines can be any connected object of the plane such as points, curves, planes, or fractals. The term “line” is thus a misnomer. In [7, 4, 12], the authors gave the following different definition of the level lines.

Definition 2 (level lines [7, 4, 12]). *Let u be an upper semicontinuous function. The level lines of u are defined as the boundaries of the connected components of the level sets $\{x \in \Omega, u(x) \leq \lambda\}$.*

Level lines thus defined are curves. It is easy to show that level lines are invariant to contrast changes (Definition 3) whether Definition 2 or Definition 1 is used. We will see, however, that Definition 1 makes level lines less robust to illumination changes.

Definition 3 (contrast change). *Let $u : \Omega \rightarrow \mathbb{R}$ and $v : \Omega \rightarrow \mathbb{R}$ be two functions. They are said to differ by a contrast change if there exists a strictly monotonic function $g : \mathbb{R} \rightarrow \mathbb{R}$ such that $u = g(v)$.*

Overall, we will see that Definition 1 should be used for the algorithms to be invariant to slight contrast changes or camera gains, while Definition 2 is preferred for large illumination deviations.

3. Level line invariance. In this section we characterize the scenes that produce illumination invariant level lines. All of the proofs of the following results are in the appendices. We first suppose that s is C^2 and α is C^1 . This implies that $u_{S,L}$ is C^1 for any $L \in \mathcal{L}$. Let us recall two important definitions of differential geometry.

Definition 4 (Gaussian curvature). *The Gaussian curvature of a surface in \mathbb{R}^3 is defined as the product of its two principal curvatures. With our notation, the Gaussian curvature of s is defined as $\det(\nabla^2 s)$.*

Definition 5 (developable surface). *A C^2 surface which has a zero Gaussian curvature on every point is called developable [33]. Simple examples of such objects are planes, cylinders, and cones. A developable surface has the following properties [33]:*

- *Each point of the surface lies on a line (the generatrix) that belongs to the surface.*
- *The plane tangent to the surface is the same on each point of the generatrix.*

3.1. The case of smooth surfaces. Given the two previous definitions, we are now able to introduce the set of smooth scenes which will be proved to generate images with illumination invariant level lines.

Definition 6. Θ *denotes the set of scenes $S = (s, \alpha)$ such that s is C^2 developable, and α is C^1 and varies only in the direction orthogonal to the generatrices of s . On points where the scene surface is planar ($\nabla^2 s = 0$), α may vary in any direction.*

We prove step by step the illumination invariance of the level lines. We first focus on local properties of the images, namely, the direction of their gradient. Many contrast invariant

algorithms rely on this feature. For instance, the authors of [22] use it for change detection, the authors of [3, 8] use it to compute dissimilarity measures between two images, and the authors of [10] use it for image registration. The following theorem (proved in Appendix A using differential geometry) characterizes the scenes for which these algorithms are fully justified.

Theorem 1. *Let $s \in C^2(\Omega)$ and $\alpha \in C^1(\Omega)$. The following statements are equivalent:*

- *Statement 1.* $\forall (L_1, L_2) \in \mathcal{L} \times \mathcal{L}, \forall x \in \Omega, \nabla u_{S, L_1}(x) \Psi \nabla u_{S, L_2}(x)$.
- *Statement 2.* $S \in \Theta$.

In other words, the direction of the gradient is an illumination invariant feature if and only if the scene belongs to Θ . Let us mention that a recent result of the same kind was obtained in [8]. The authors show that the direction of the gradient is almost illumination invariant in the sense that its distribution w.r.t. the light orientation is concentrated along a given vector for most scenes.

Now let us focus on the results concerning the level line invariance. The previous result allows us to easily show the following corollary.

Corollary 1. *The level lines are illumination invariant only if the scene belongs to Θ .*

However, not all of the scenes belonging to Θ have illumination invariant level lines. For instance, Figure 3 shows a cone with constant albedo. If the directed light comes exactly in the direction of the cone axis (left), the cone radiometry is uniform and the image of the cone is composed of only one level line. In general (right), the level lines correspond to the cone generatrices.

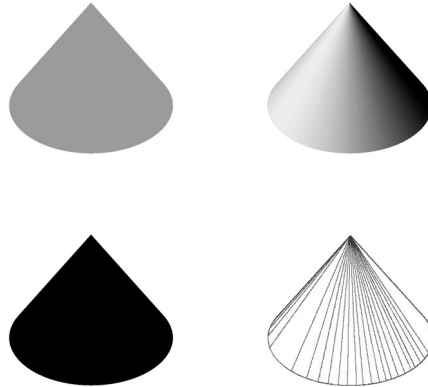


Figure 3. *Top: images of a cone illuminated using two different incident light directions. Bottom: some of their level lines.*

We can state a weaker result (proved in Appendix B using elements of topology) that completes Corollary 1.

Theorem 2. *Let $S \in \Theta$. For almost all pairs of lighting conditions $(L_1, L_2) \in \mathcal{L} \times \mathcal{L}$ (w.r.t. the Lebesgue measure of $\mathbb{R}^4 \times \mathbb{R}^4$), the level lines of u_{S, L_1} are the same as those of u_{S, L_2} .*

This theorem and Corollary 1 show that there is “almost” an equivalence between the following statements:

- The scene has invariant level lines.

- The scene belongs to Θ .

Finally, let us stress that, using Definition 1, no surface—except the planes—would lead to illumination invariant level lines.

3.2. The case of nonsmooth surfaces. Unfortunately, the space Θ contains too few surfaces to model any real-life scene.¹ This leads us to analyze the level line invariance when S is a piecewise developable C^2 mapping with its albedo varying orthogonally to the generatrices on each piece. Let us give a precise definition of this space.

Definition 7 (Ξ). Ξ is the space of scenes $\bar{S} = (\bar{s}, \bar{\alpha})$ such that there exist a finite set $\{\omega_i\}_{i \in I}$ and a scene $S = (s, \alpha)$ which satisfy the following:

- $\forall i \in I, \omega_i \subset \Omega$ is an open, nonempty connected set.
- $\forall (i, j), \omega_i \cap \omega_j = \emptyset$.
- $\cup_{i \in I} \bar{\omega}_i = \Omega$.
- $\forall i, S|_{\omega_i} \in \Theta$ (the restriction of S to ω_i belongs to Θ).
- Finally, we suppose that $S|_{\omega_i}$ (as well as $N|_{\omega_i}$) admits a limit on the boundary of ω_i . This allows us to define $\bar{S} = (\bar{s}, \bar{\alpha})$ everywhere. For instance, we can define it this way:

$$\begin{cases} (\bar{s}, \bar{\alpha})(\mathbf{x}) = (s, \alpha)(\mathbf{x}) & \text{if } \mathbf{x} \in \cup_{i \in I} \omega_i, \\ \begin{cases} \bar{s}(\mathbf{x}) = \lim_{r \rightarrow 0} \sup_{\mathbf{y} \in B(\mathbf{x}, r)} s(\mathbf{y}) \\ \bar{\alpha}(\mathbf{x}) = \lim_{r \rightarrow 0} \sup_{\mathbf{y} \in B(\mathbf{x}, r)} \alpha(\mathbf{y}) \end{cases} & \text{otherwise.} \end{cases}$$

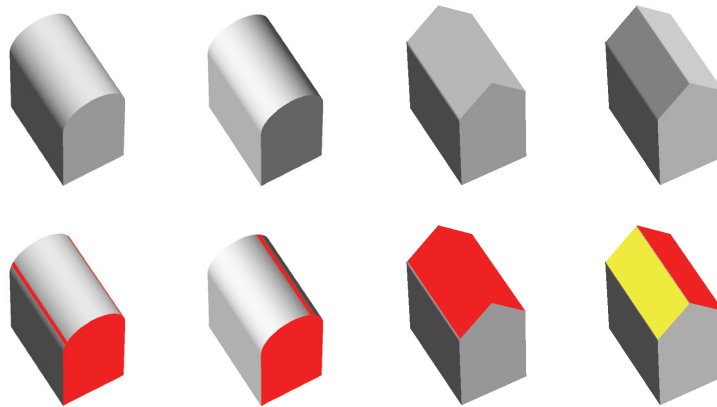


Figure 4. Examples of noninvariance of the level lines in the nonsmooth case. The colored parts represent singular level lines.

For images generated from scenes in Ξ , the level lines have weaker invariance properties than in the case of smooth surfaces. Figure 4 illustrates this fact. On the four objects on the

¹This holds with the exception of warped documents. A warped sheet of paper is developable. This is an alternative definition of the developable surfaces. Theorem 2 could thus be used for the task of document unwarping, independently of the lighting conditions. This remark has already been made by some authors [9, 34, 38].

left, most of the level lines of the cylinder-shaped roof are just segments on the roof. Depending on the light orientation, one or two of these segments can merge with the “building wall.” Consequently, the level lines are noninvariant. The four objects on the right of Figure 4 show the image of a triangle-shaped roof under two different illuminations. This roof is composed of two plane portions. If the light direction belongs to the plane bisecting these portions, then they will have the same radiosity. For most light orientations, the roof will thus be constituted of two level lines (yellow and red), while for a set of zero measure, it can be constituted of only one level set (red). In the following we state those observations in a formal way.

Proposition 1. *Let S belong to Ξ . Let $\omega_i = p(\omega_i)$ and $\omega_j = p(\omega_j)$ be adjacent pieces. Two adjacent level lines of $u_{S,L}|_{\omega_i}$ and $u_{S,L}|_{\omega_j}$ merge for almost no L .*

This proposition allows to show the following simple result.

Corollary 2. *Let S be a piecewise planar surface with constant albedo on each piece. The level lines of $u_{S,L}$ are the same for almost every L .*

This result concludes the theoretical part of this article.

4. An illumination invariant algorithm for change detection. With the previous results in mind, we turn to the problem of change detection. The detection of changes between two grayscale images is a very challenging problem. Some recent theoretical results show that it is in some sense unsolvable. It is indeed impossible (under the Lambertian assumption) to decide whether two images represent the same object or different objects under different illuminations [8]. In practice—to the best of our knowledge—no algorithm is yet able to treat large remotely sensed images of urban areas with a reasonable number of false positives. The main difficulties that arise in designing such an algorithm are the changes in illumination, the profusion of details in high resolution images, the parallax errors (see Figure 5), and a large number of minor changes that should not be detected. All of these difficulties have led some authors to set aside the details provided by high resolution images and to concentrate only on major changes of the urban landscape [22].

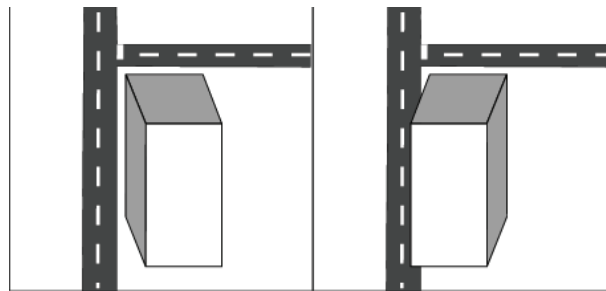


Figure 5. *Illustration of parallax errors: Two identical scenes are rendered with different geometries.*

However, humans are able to perform change detection manually (though some situations are ambiguous) at the cost of a large amount of time. It thus seems possible to achieve—or at least assist in—this task using automatic algorithms. Humans often require some semantic interpretation of the scene to detect changes. It is thus necessary to introduce some priors about the scene geometry. For instance, some authors try to find objects whose boundaries are lines or polygons [21, 19, 11] as these are likely to be buildings. Other authors assume that

the scene elevation is piecewise constant [39]. In this work, we make the assumption that the scene belongs to Ξ . We propose a simple algorithm that equalizes the contrast of two images. After this step, a simple per-pixel difference followed by a thresholding gives encouraging results on both synthetic OpenGL images and real QuickBird images. The synthetic images were designed in order to illustrate the theoretical results obtained in this work.

4.1. Underlying assumptions. Let us recall and justify the following assumptions on the scenes:

Assumption 1. The surfaces have Lambertian reflectance.

Assumption 2. The lighting is a mixture of ambient light and directional light.

Assumption 3. The scene belongs to Ξ (see Definition 7).

Assumption 4. The two pictures are registered exactly.

Assumption 5. For the time being, we assume that there are no shadows.

- Assumption 1 approximately holds as most city surfaces are rough (concrete, asphalt, etc.). Cases where this hypothesis would not hold are cases such as wet tile or glass roofs which have a strong specular component.
- Assumption 2 is natural as there only is a punctual source of light at infinity (the sunlight). It can create ambient light due to diffusion of the sunlight in the atmosphere and reflections on the ground.
- Assumption 3 relies on the geometrical structure of urban scenes. It is more difficult to describe, as different regions of the world might have different kinds of constructions. Nevertheless, most buildings have a common characteristic: our claim is that they are generally piecewise developable. Hemispherical roofs are very rare. Figure 6 is part of a collection of roofs used in [18], where the authors create a dictionary of shapes corresponding to portions of European-style buildings. They all satisfy this assumption.
- Assumption 4 is a strong assumption. In practice two airborne or satellite images are seldom taken from exactly the same position. This introduces parallax errors as depicted in Figure 5. Reducing these issues requires nonrigid registration techniques. They are still under development, with interesting perspectives (see, for instance, [10, 17, 23]). In our experiments we applied only rigid registration, which explains some false positives.
- To simplify the discussion, we will deal with shadows later on. This means that the directional light lies everywhere in the scene.

4.2. A contrast equalization algorithm. Under the previous assumptions we saw that the level lines of urban area images should be “almost” invariant to illumination changes. We propose a contrast enhancement and a change detection procedure that take advantage of this result. Let u_1 and u_2 be two exactly registered images taken under different lighting conditions L_1 and L_2 at times t_1 and t_2 . Let S be the 3D scene at time t_1 . Under these assumptions we can write

$$(4.1) \quad \begin{cases} u_1 = u_{S,L_1}, \\ u_2 = u_{S,L_2} + c_{1,2}, \end{cases}$$

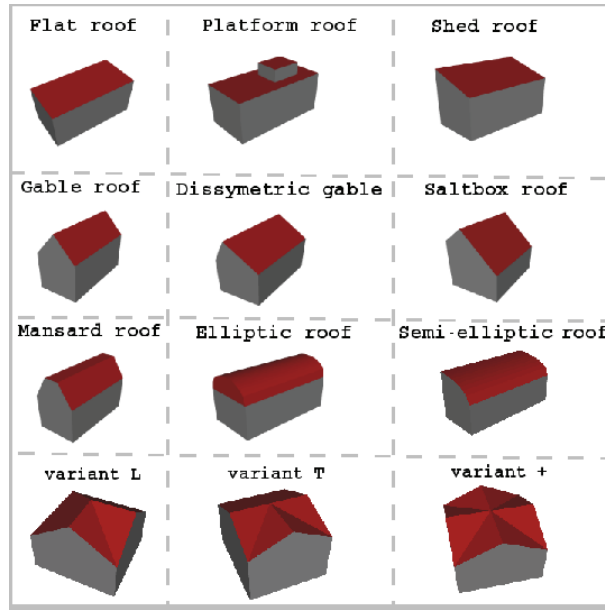


Figure 6. Dictionary of roofs. Courtesy of F. Lafarge, INRIA, Sophia-Antipolis, France.

where $c_{1,2}$ denotes the changes from image u_1 to image u_2 . In this equation u_{S,L_2} and $c_{1,2}$ are unknown. To retrieve them, we need to introduce priors. From the previous discussion, it is natural to consider that u_{S,L_2} should belong to the space of images which have the same level lines as u_1 . We denote this space χ_{u_1} . We can also devise a prior $J(c)$ on the changes. In most applications, the changes are sparse. In this article, as the L^1 -norm is well known to favor sparse structures, we simply set $J(c) = \|c\|_1$. To retrieve $c_{1,2}$ we can thus solve the problem

$$(4.2) \quad \inf_{u \in \chi_{u_1}} (\|u_2 - u\|_1)$$

and set $c_{1,2} = u_2 - \bar{u}$, where \bar{u} is the solution of (4.2). Problem (4.2) can be reformulated as follows: “find the image u closest to u_2 which has the same level lines as u_1 .” It is therefore a problem of contrast equalization.

To solve (4.2) we need to discretize χ_{u_1} . We propose the following simple strategy:

1. Set $u_Q = \lfloor \frac{u_1}{\Delta} \rfloor \Delta$ (uniform quantization).
2. For each level $k\Delta$ ($k \in \mathbb{Z}$), separate the connected components $\Omega_{k,j}$ of the set $\Omega_k = \{x \in \mathbb{R}^n, u_Q(x) = k\Delta\}$. In the experiments, we use the 8-neighborhood to define the notion of connected component.

Note that the sets $\Omega_{k,j}$ were referred to as *bilevel lines* in [1]. We define χ_{u_1} as the set of images that are constant on each bilevel line. With this definition, the solution of (4.2) is in closed form:

$$(4.3) \quad \bar{u}|_{\Omega_{k,j}} = \text{median}(u_2|_{\Omega_{k,j}}).$$

The image of the changes is $c_{1,2} = u_2 - \bar{u}$. This image should be nonzero only on level lines

where changes occurred. In practice, as the piecewise developable model is only an approximation, a threshold is applied in order to detect the changes' support. In the experiments of Figure 7, for instance, we set the color as red if $c_{1,2} > \delta$, where δ is a user-defined parameter.

This kind of algorithm has already been used and analyzed with a different motivation in [5]. This is a very fast algorithm (less than 0.4 second for a 1000×1000 image on an Intel Xeon CPU at 1.86GHz). Let us mention that it shares many similarities with what is proposed in [1]. In that paper, the authors first split the image into the set of its bilevel lines and then compare them pairwise using geometric measures. This algorithm has the drawback of being more computationally intensive. The main drawback of our proposed procedure is that it makes use of a thresholding on image intensity, which is not an invariant feature.

Finally, let us point out that our algorithm is nonsymmetric. We can solve the problem

$$(4.4) \quad \inf_{u \in \chi_{u_2}} (\|u_1 - u\|_1)$$

and retrieve another change image $c_{2,1} = u_1 - \bar{u}$. In general we obtain $c_{1,2} \neq c_{2,1}$. This is a useful feature which allows us to determine which scene contains a given detected object (see Figure 7). If one is interested in getting all the differences between the two objects, then one may use the decision rule $|c_{1,2}| + |c_{2,1}| > \delta$.

4.3. Robustness to noise and parameters. The algorithm—as described in the previous section—depends on two explicit parameters (the quantization step Δ and the threshold δ) and on one implicit offset parameter, $\epsilon \in [0, \Delta[$. The offset parameter can be used to redefine u_Q as follows: $u_Q = \lfloor \frac{u_1 + \epsilon}{\Delta} \rfloor \Delta$. In practice, it has little effect on the results, and we always set it to 0.

The parameters Δ and δ play an important role and should be chosen depending on the image quality. For synthetic images such as those presented in Figure 7 they can be chosen very small. In this test case, the pixel intensities vary in the interval $[0, 255]$, and we simply set $\Delta = \delta = 1$.

In real test cases like those presented in Figures 8 and 9, this strategy would not provide decent results. Indeed, the level lines as defined in Definition 2 are not stable w.r.t. small perturbations. For instance, a flat scene should be represented by a constant image and thus be constituted of only one level line. However, by adding noise to the image or an arbitrarily small perturbation to the scene elevation, the level lines can become arbitrary sets. The Δ parameter can be used in order to stabilize the level line extraction:

- For uniform noise, Δ and δ should be chosen equal to the noise amplitude.
- For nonbounded noises, we decided to denoise/decompose the images first, using a total variation algorithm. Then in all experiments $\Delta = \delta$ were chosen by hand. Note that these parameters are very easy to tune since the algorithm output is obtained in real time.

5. Results. In this section, we compare our approach with two classical algorithms, namely, the monotone projection [26] and the change detection using the fast level set transform (FLST) [28]. We choose these algorithms as both are asymmetric. The first is a fundamental tool of image processing, while the second is based on principles similar to ours. We briefly describe them and then compare them on synthetic and real data.

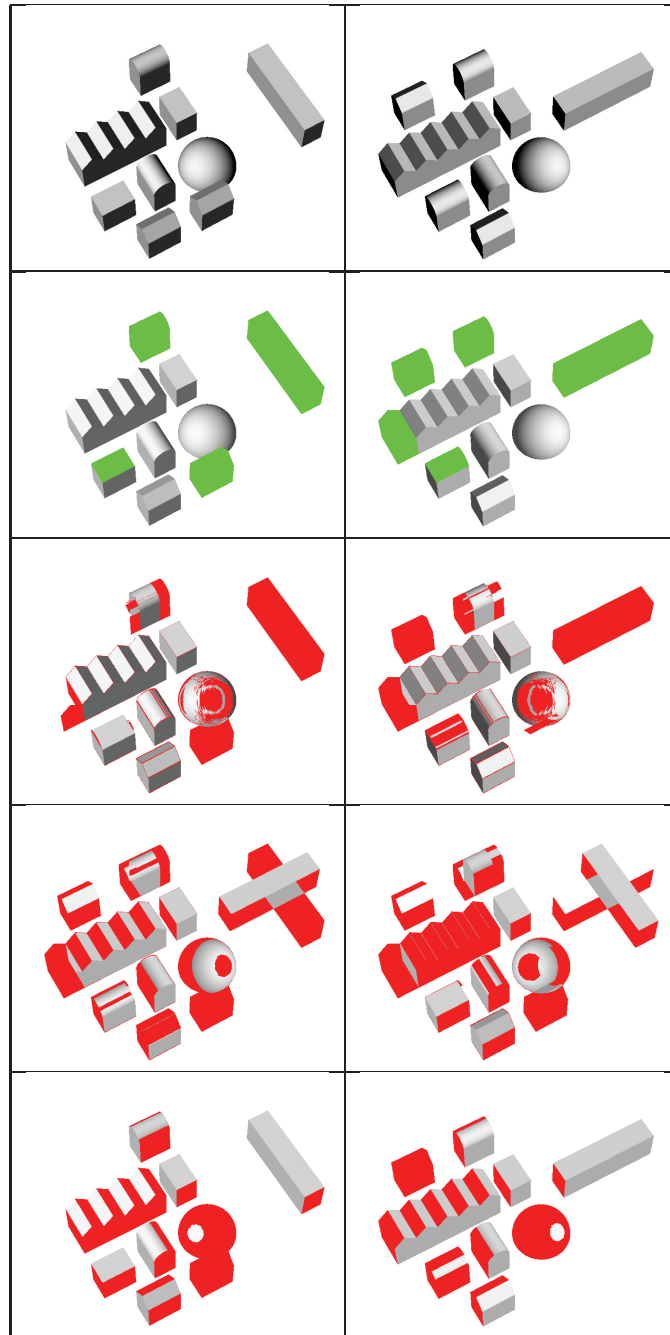


Figure 7. Toy example. First row: two images under different lighting conditions with some changes. Second row: the changes are depicted in green (ground truth). Third row: change detection using our algorithm. Fourth row: change detection using a least squares contrast equalization. Fifth row: change detection using the FLST.

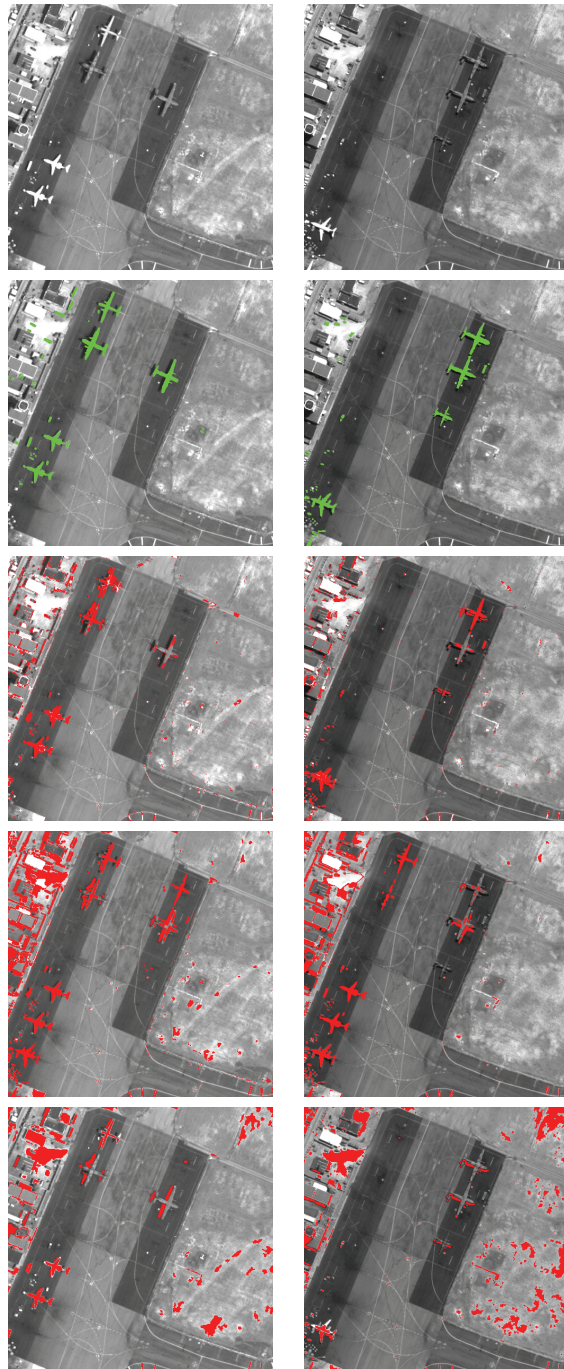


Figure 8. QuickBird images (61cm resolution) of Abidjan airport. First row: Airport on 04/02/2003 and 07/07/2003. Second row: ground truth (the changes are depicted in green). Third row: change detection using our algorithm. Fourth row: change detection using a least squares contrast equalization. Fifth row: change detection using the FLST. Copyright CNES, distribution Spot Image.

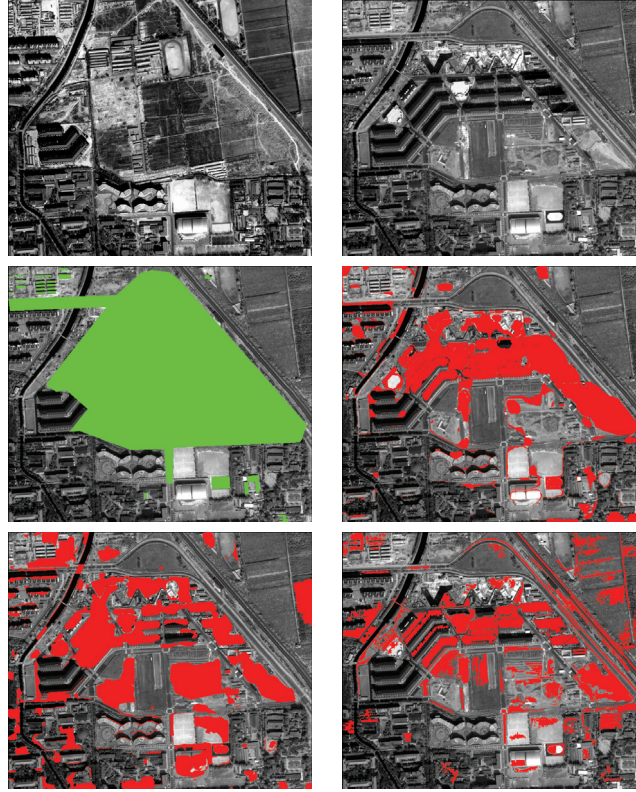


Figure 9. QuickBird images (61cm resolution) of Beijing. First row: Beijing in 2001 (left) and 2003 (right). Second row: ground truth with the changes depicted in green (left) and change detection using our algorithm (right). Third row: change detection using a monotone projection (left) and change detection using the FLST (right). Images kindly provided by the RSIU team at Liama Laboratory, Beijing, China.

5.1. Description of alternative approaches.

5.1.1. Monotone projection. The monotone projection is described in [26]. It is similar to a global contrast equalization. We choose it for comparison as it is more general than a linear contrast equalization [31, 41]. As in section 4.2, we suppose that we have two images that can be written as

$$(5.1) \quad \begin{cases} u_1 = u_{S,L_1}, \\ u_2 = u_{S,L_2} + c_{1,2}. \end{cases}$$

The principle of the monotone projection is to assume that two images of the same scene taken under different illuminations differ only by a global monotonic contrast change. This means that $u_{S,L_2} = g \circ u_{S,L_1}$, where $g : \mathbb{R} \rightarrow \mathbb{R}$ is a nondecreasing function. To retrieve the changes we can therefore find the function \bar{g} which minimizes the following energy:

$$(5.2) \quad \bar{g} = \arg \min_{g \text{ nondecreasing}} (\|g \circ u_1 - u_2\|_2^2).$$

Finally, we set $c_{1,2} = \bar{g} \circ u_1 - u_2$. Problem (5.2) can be solved in $O(n)$ operations, where n is the number of pixels [26].

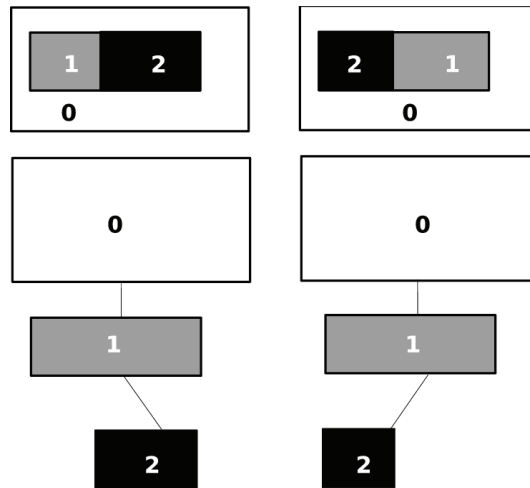


Figure 10. *Top: images of a “triangle”-shaped roof under different illuminations. Bottom: FLST of each image.*

5.1.2. Comparison of the level set trees. Monasse and Guichard [28] propose a contrast invariant algorithm for change detection. This algorithm is close to ours since it makes extensive use of the level lines.

The algorithm principle is the following: first, each image is decomposed into a tree of “shapes” (the connected components of the image level sets). Figure 10 shows the FLST of two different functions. The two trees are then compared. A shape in the tree of u_1 will be said to match in the tree of u_2 if there exists a shape in this tree that has approximately the same moments (position, area, etc.). In Figure 10, the nonmatching shapes would be the shapes labeled “2.” The change images $c_{1,2}$ and $c_{2,1}$ are then recomposed from the nonmatching shapes. We refer the reader to [28, 1] for more details about this method.

5.2. Synthetic images. To outline the results presented in this article, we devised a simple 3D scene generator which allows one to visualize simple instances of cities under different lighting conditions. The top images in Figure 7 show two images of “urban” areas. In this example, some buildings appeared or disappeared, the shape of some elements changed, and some buildings moved.

In this toy example, the scene does not belong to Ξ (one of the buildings is a dome), but all the other hypotheses of our model are satisfied. It illustrates our previous discussions on illumination invariance:

- The output of the monotone projection algorithm is not satisfactory. A global monotonic contrast change cannot reproduce local grayscale inversions. This explains the many false positives on the triangle rooftops.
- The output of the FLST algorithm is not satisfactory either. The reason is twofold. First, in our experiments we compare shapes using only their barycenters and their areas. Such a measure is too naive to give satisfactory results. In [28], the authors suggest using higher order moments. However, this makes parameter evaluation more difficult and computation times higher.

Moreover, the method should fail even with a good measure of comparison because the level set transform is not illumination invariant: a locally nonzero curvature can be responsible for local contrast inversions and completely change the inclusion tree. For example, Figure 10 shows an image of a triangle-shaped roof under two different illuminations. We can see that the level set trees are different. When comparing the two images, the shapes labeled “2” cannot match. Those shapes will thus be evaluated as changed by the algorithm.

- The output of our algorithm is satisfactory on this toy example. It fails on the dome (Gaussian curvature is not null) for a few level lines and for the top cylinder-shaped building. This is expected since the dome is not developable and the level lines are only “almost” invariant. Between the two shots, the top cylinder-shaped building moves along its axis; only the nonoverlapping parts of it are detected as changed.

5.3. Natural images. Let us now turn to real images. Our assumptions on the scene surface are met only at large scales. Roof tiles, for instance, might have a nonzero local curvature, whereas the roof considered in its whole is usually planar. To apply the previous algorithm, we thus begin with a fast cartoon+texture decomposition algorithm [40] and work only on the cartoon parts. In the following experiments we simply used the Rudin–Osher–Fatemi model [32]. Furthermore, we have not considered shadows in our model. Shadowed regions are only lightened by ambient light. Their intensity can generally be considered as a tenth of the regions lightened by directed light [39]. We thus remove the changes due to shadows by not considering the changes with low intensity. Note that there exist more advanced techniques for removing shadows [14].

We provide comparisons on two pairs of QuickBird images. All the methods depend on a thresholding parameter. We thus provide ROC curves to compare the performances of the algorithms when the thresholds vary. Note that we defined the ground truth by hand for the following two sets of images:

- *Airport of Abidjan.* On this image, the changes are quite easy to detect. All algorithms perform well.

Compared with a classical approach (i.e., global contrast equalization followed by a per-pixel difference; see Figure 8, bottom left), our algorithm yields satisfactory results, with few false negatives and many fewer false positives in very short times (3 seconds for the presented image). Our implementation of the FLST does not yield satisfactory results compared with the other approaches. This might be due to the fact that we compare shapes using only their barycenters and areas. As mentioned before, results can be improved by using higher order moments, but this increases the complexity of the parameter evaluation. This problem is important as the shapes matching algorithm takes around 30 seconds.

The ROC curves (see Figure 11) show a good behavior of our algorithm. For this pair of images, we can obtain 85% true positives with only 5% false positives, whereas the other algorithms generate more than 20% false positives to achieve the same rate of true positives. We can see that additional decision rules should be added to get a perfect result, but in this state, the algorithm can be considered as a good elementary classifier. The main reason for failure of our algorithm is the problem of registration: some painted lines on the taxiway are not exactly registered, and some buildings’ edges do

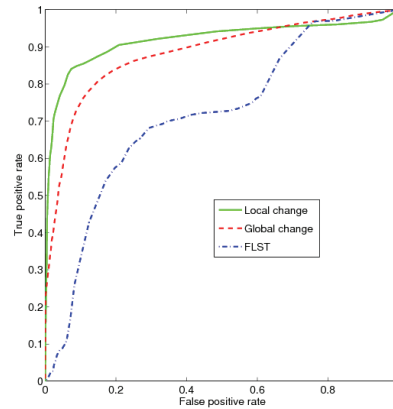


Figure 11. ROC curves for Abidjan airport.

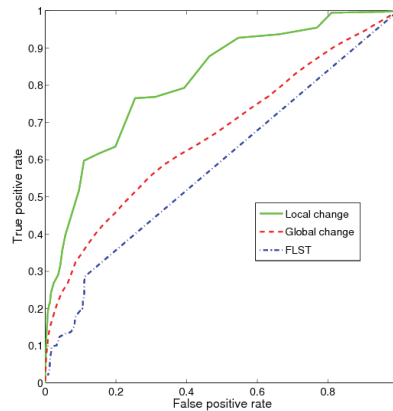


Figure 12. ROC curves for Beijing suburb.

not coincide. Some false positives occur due to seasonal changes in the vegetation surrounding the taxiway.

- *City of Beijing*. This pair of pictures is more challenging than the previous one. Huge modifications of the landscape occurred between the two shots. Only a coarse ground truth can be obtained. Our algorithm still gives satisfactory results: very few false positives are obtained, and a large number of the changes are detected. With a correctly chosen threshold, we obtain 75% true positives and only 25% false positives. The other methods yield many false positives, and their output seems difficult to use (see the ROC curves in Figure 12).

Conclusion. In this work we characterized the scenes that produce images with illumination invariant level lines. Based on this result, we proposed a contrast equalization and change detection algorithm. This simple and fast algorithm gives good results. Designing

more precise change detection algorithms would require further semantic interpretation of the scenes. We hope that our theoretical contribution and practical experiment will encourage other researchers to use the level lines in more complex frameworks.

The next sections contain all of the proofs of the propositions and theorems stated in this paper.

Appendix A. Proof of Theorem 1.

Proof. Let us first express the gradient of u in terms of (s, α) and (l, γ) . Simple geometry leads to $\mathbf{N}(\mathbf{x}) = \Psi(\nabla s(\mathbf{x})) = \frac{(-s_1(\mathbf{x}), -s_2(\mathbf{x}), 1)}{\sqrt{s_1^2(\mathbf{x}) + s_2^2(\mathbf{x}) + 1}}$, where s_1 and s_2 are the derivatives of s along the two axes of the object plane. Let $\mathbf{x} = p^{-1}(x)$. Using the chain rule and (2.2), we get that

$$\nabla u_{S,L}(x) = \left(\underbrace{l}_{\in \mathcal{M}_{1,3}} \cdot \left[\underbrace{\Psi'(\nabla s(\mathbf{x}))}_{\in \mathcal{M}_{3,2}} \cdot \underbrace{\nabla^2 s(\mathbf{x})}_{\in \mathcal{M}_{2,2}} \underbrace{\alpha(\mathbf{x})}_{\in \mathbb{R}} + \underbrace{\Psi(\nabla s(\mathbf{x}))}_{\in \mathcal{M}_{3,1}} \cdot \underbrace{\nabla \alpha(\mathbf{x})}_{\in \mathcal{M}_{1,2}} \right] + \underbrace{\gamma \nabla \alpha(\mathbf{x})}_{\in \mathcal{M}_{1,2}} \right) \cdot \underbrace{J(p^{-1})(x)}_{\in \mathcal{M}_{2,2}}.$$

This can be rewritten as

$$(A.1) \quad \nabla u_{S,L}(x) = (l \cdot A(\mathbf{x}) + \gamma \nabla \alpha(\mathbf{x})) \cdot J(p^{-1})(x)$$

with

$$(A.2) \quad A(\mathbf{x}) = \left([M_1, M_2] \cdot \begin{bmatrix} s_{11} & s_{12} \\ s_{12} & s_{22} \end{bmatrix} + \mathbf{N} \cdot [\alpha_1, \alpha_2] \right) (\mathbf{x}).$$

$M_1(\mathbf{x}), M_2(\mathbf{x}) \in \mathcal{M}_{3,1}$ are the two columns of $\Psi'(\nabla s(\mathbf{x}))\alpha(\mathbf{x})$ and $\mathbf{N}(\mathbf{x}) = \Psi(\nabla s(\mathbf{x}))$.

We give the preliminaries to show *Statement 1* \Rightarrow *Statement 2*. Let S be a scene such that

$$(A.3) \quad \forall (L_1, L_2) \in \mathcal{L} \times \mathcal{L}, \quad \forall x \in \Omega, \quad \nabla u_{S,L_1}(x) \Psi \nabla u_{S,L_2}(x).$$

Let $D : \Omega \rightarrow \mathbb{S}^2$ denote the invariant direction of $\nabla u_{S,L}$. On points x where $\forall L \in \mathcal{L}, \nabla u_{S,L}(x) = 0$, D might denote any vector in \mathbb{R}^2 .

As (A.3) must be true $\forall ([l_1, \gamma_1], [l_2, \gamma_2]) \in \mathcal{L} \times \mathcal{L}$, it needs to be true for $\gamma_1 = \gamma_2 = 0$. We thus drop the term $\gamma[\alpha_X, \alpha_Y]$ in (A.1). Relation (A.3) can be rewritten as

$$(A.4) \quad \forall l \in \mathcal{L}, \quad \forall x \in \Omega, \quad l \cdot A(\mathbf{x}) \cdot J(p^{-1})(x) \Psi D(x).$$

As p is a diffeomorphism, $J(p^{-1})(x)$ is a nonsingular 2 by 2 matrix. Thus property (A.4) does not depend upon $J(p^{-1})$ and is true only if the matrix $A(\mathbf{x})$ has two parallel rows. This can be rewritten as

$$(A.5) \quad \begin{cases} (s_{11}M_1 + s_{12}M_2 + \alpha_1\mathbf{N})(\mathbf{x}) = a(\mathbf{x})C(\mathbf{x}), \\ (s_{12}M_1 + s_{22}M_2 + \alpha_2\mathbf{N})(\mathbf{x}) = b(\mathbf{x})C(\mathbf{x}), \end{cases}$$

where $(a, b) : \Omega \rightarrow \mathbb{R}^2$ and $C : \Omega \rightarrow \mathcal{M}_{3,1}$ are C^0 mappings. Some elementary (but fastidious) calculus leads to $\det([M_1, M_2, \mathbf{N}](\mathbf{x})) > 0$ so that the vectors $M_1(\mathbf{x}), M_2(\mathbf{x}), \mathbf{N}(\mathbf{x})$ form a basis of \mathbb{R}^3 . System (A.5) thus implies that

$$(A.6) \quad \begin{pmatrix} s_{11} \\ s_{12} \\ \alpha_1 \end{pmatrix} (\mathbf{x}) \Psi \begin{pmatrix} s_{12} \\ s_{22} \\ \alpha_2 \end{pmatrix} (\mathbf{x})$$

so that

$$(A.7) \quad \begin{pmatrix} s_{11} \\ s_{12} \end{pmatrix}(\mathbf{x}) \Psi \begin{pmatrix} s_{12} \\ s_{22} \end{pmatrix}(\mathbf{x}) \Psi \begin{pmatrix} \alpha_1 \\ \alpha_2 \end{pmatrix}(\mathbf{x}).$$

Finally (A.7) leads to $\forall \mathbf{x} \in \Omega, \det(\nabla^2 s(\mathbf{x})) = 0$, which means that s is developable. It is easy to check that the eigenvector of $\nabla^2 s(\mathbf{x})$ is $\begin{pmatrix} s_{12} \\ s_{22} \end{pmatrix}(\mathbf{x})$. This eigenvector is in the direction orthogonal to the generatrix of s passing through point \mathbf{x} . Equation (A.7) thus indicates that $\alpha(\mathbf{x})$ varies in the direction orthogonal to this generatrix. For points such that $\nabla^2 s(\mathbf{x}) = 0$, no condition is imposed on $\alpha(\mathbf{x})$.

Now let us prove *Statement 2* \Rightarrow *Statement 1*. Let $S = (s, \alpha) \in \Theta$. This implies that $\forall \mathbf{x} \in \Omega, \det(\nabla^2 s(\mathbf{x})) = 0$. Thus there exists $(c_1, c_2, a, b) : \Omega \rightarrow \mathbb{R}^4$ such that

$$(A.8) \quad \begin{bmatrix} s_{11} & s_{12} \\ s_{12} & s_{22} \end{bmatrix} = \begin{bmatrix} c_1 a & c_2 a \\ c_1 b & c_2 b \end{bmatrix}$$

with $c_1 b = c_2 a$. Moreover, by hypothesis, the gradient varies orthogonally to the generatrices, so that there exists c_3 such that

$$(A.9) \quad [\alpha_1, \alpha_2] = c_3 [a, b].$$

Using (A.8) and (A.9), the matrix A (A.2) can be rewritten as

$$(A.10) \quad A = [aC, bC]$$

with $C = M_1 c_1 + M_2 c_2 + N c_3$ so that (A.1) simplifies to

$$(A.11) \quad \nabla u_{S,L}(x) = (\langle l, C \rangle + \gamma c_3 [a, b]) (\mathbf{x}) \cdot J(p^{-1})(x),$$

and thus $\nabla u_{S,L}(x) \Psi [a, b](\mathbf{x}) \cdot J(p^{-1})(x) \forall L \in \mathcal{L}$. ■

Appendix B. Proof of Theorem 2. In the following we prove Theorem 2. In order to do so, we first need some preliminary lemmas.

Lemma 1. *Let $C : \Omega \rightarrow \mathbb{R}_*^4$ be a mapping (no regularity assumption is made). Let $L \in \mathcal{L}$; then L^\perp denotes the hyperplane orthogonal to L . Let $\omega_L = \text{int}(\{x \in \Omega, C(x) \in L^\perp\})$. For almost every $L \in \mathcal{L}$ (w.r.t. the Lebesgue measure of \mathbb{R}^4) $\omega_L = \emptyset$.*

Proof. Let us denote $Y = \{L \in \mathcal{L}, \omega_L \neq \emptyset\}$. Let $\Omega_{\mathbb{Q}} = \{\mathbb{Q}^2 \cap \Omega\}$. Since $\Omega_{\mathbb{Q}} \subset \mathbb{Q}^2$, $\Omega_{\mathbb{Q}}$ is a countable set.

Let $a_i \in \Omega_{\mathbb{Q}}$ and $Y_i = \{L \in \mathcal{L}, a_i \in \omega_L\}$. Y_i is a subset of a hyperplane of \mathbb{R}^4 . If that were not the case, there would exist four elements of Y_i , L_1, L_2, L_3, L_4 , that would form a basis of \mathbb{R}^4 . As $C(a_i) \perp L_j \forall j \in \{1, 2, 3, 4\}$, it would mean that $C(a_i) = 0$, which contradicts $C(a_i) \in \mathbb{R}_*^4$.

Thus $\mu_{\mathbb{R}^4}(Y_i) = 0$ and $\mu_{\mathbb{R}^4}(\bigcup_{a_i \in \Omega_{\mathbb{Q}}} Y_i) = 0$. Furthermore $\bigcup_{a_i \in \Omega_{\mathbb{Q}}} Y_i = Y$ (since each nonempty open set ω_L contains an element of \mathbb{Q}^2). Therefore, $\mu_{\mathbb{R}^4}(Y) = 0$. ■

Lemma 2. *Let $\omega \in \Omega$ be an open set. Let u_1 and u_2 be two $C^1(\Omega)$ functions such that $\forall x \in \Omega, \nabla u_1(x) \Psi \nabla u_2(x), \nabla u_1(x) \neq 0$, and $\nabla u_2(x) \neq 0$. Then u_1 and u_2 have the same level lines on ω .*

Proof. As ∇u_1 and ∇u_2 are nonzero on ω , the implicit functions theorem states that level lines of u_1 and u_2 are C^1 curves. Moreover, the curves can be defined based only on using their respective normals, $\frac{\nabla u_1}{|\nabla u_1|}$ and $\frac{\nabla u_2}{|\nabla u_2|}$, which are equal. ■

Lemma 3. *Let u_1 and u_2 be two $C^1(\Omega)$ functions such that*

$$\forall x \in \Omega, \quad \nabla u_1(x) \Psi \nabla u_2(x).$$

Let

$$\Omega_1^0 = \{x \in \Omega, \nabla u_1(x) = 0\} \quad \text{and} \quad \Omega_2^0 = \{x \in \Omega, \nabla u_2(x) = 0\}.$$

The following statements are equivalent:

- *Statement 1.* u_1 and u_2 have the same level lines.
- *Statement 2.* $\overset{\circ}{\Omega}_1^0 = \overset{\circ}{\Omega}_2^0$.

Proof. *Statement 1* \Rightarrow *Statement 2* is straightforward.

We prove this by contradiction. Let us suppose that $\overset{\circ}{\Omega}_1^0 \neq \overset{\circ}{\Omega}_2^0$. In this case, up to an index inversion, there exists an open set ω such that $\nabla u_1 = 0$ on ω and $\nabla u_2 \neq 0$. u_1 is constant on ω and is thus included in a level line of u_1 , whereas $\nabla u_2 \neq 0$ implies that $\exists(x, y) \in \omega^2$ such that $u_2(x) \neq u_2(y)$. Therefore ω is not included in a level line of u_2 , and we can conclude that u_1 and u_2 do not have the same level lines.

Let $\tilde{\Omega}^+ = \Omega \setminus \overline{\overset{\circ}{\Omega}_1^0}$. In order to prove that *Statement 2* \Rightarrow *Statement 1*, we proceed as follows. We show that the level lines of u_1 and u_2 restricted to $\tilde{\Omega}^+$ and to $\overline{\overset{\circ}{\Omega}_1^0}$ are the same. This allows us to conclude that the level lines are the same on the whole domain Ω . We detail this reasoning below.

1. *The level lines are the same on $\tilde{\Omega}^+ = \Omega \setminus \overline{\overset{\circ}{\Omega}_1^0}$.*

Let $\omega \subset \Omega$ be an open set such that $\nabla u_1 = 0$ on ω . Necessarily $\omega \subset \overset{\circ}{\Omega}_1^0$, and thus $\omega \cap \tilde{\Omega}^+ = \emptyset$. Let $\Omega_1^+ = \{x, \nabla u_1(x) \neq 0\}$ and $\Omega_2^+ = \{x, \nabla u_2(x) \neq 0\}$. Ω_1^+ and Ω_2^+ are open due to the continuity of ∇u_1 and ∇u_2 . Furthermore, the previous reasoning allows us to conclude that Ω_1^+ and Ω_2^+ are dense sets in $\tilde{\Omega}^+$. Therefore $\Omega_1^+ \cap \Omega_2^+$ is a dense open set in $\tilde{\Omega}^+$ as the intersection of two dense open sets.

From Lemma 2, we know that the level lines of u_1 and u_2 are the same on $\Omega_1^+ \cap \Omega_2^+$.

The continuity of u_1 and u_2 ensures that they are also the same on $\overline{\Omega_1^+ \cap \Omega_2^+} = \tilde{\Omega}^+$.

2. *The level lines are the same on $\overline{\overset{\circ}{\Omega}_1^0}$.*

By definition, ∇u_1 and ∇u_2 are zero on $\overset{\circ}{\Omega}_1^0 = \overset{\circ}{\Omega}_2^0$. This can be extended by continuity to $\overline{\overset{\circ}{\Omega}_1^0}$. Therefore u_1 and u_2 are both constant on each connected component U_i of $\overline{\overset{\circ}{\Omega}_1^0}$.

Every connected component U_i is thus a level line of u_1 and u_2 on $\overline{\overset{\circ}{\Omega}_1^0}$.

3. *The level lines are the same on Ω .*

Let us now consider a level line A of u_1 (and u_2) in $\overline{\tilde{\Omega}^+}$. Then one of the following holds:

- $\forall i, U_i \cap A = \emptyset$, in which case, from the previous discussion, A is a level line of u_1 and u_2 in Ω .
- $\exists i, U_i \cap A \neq \emptyset$. Then $A \cup U_i$ is a connected set. With u_1 being continuous and constant on U_i and A , we get that u_1 is constant on $A \cup U_i$. Similarly, u_2 is constant on $A \cup U_i$, and thus $A \cup U_i$ is a subset of a level line of u_1 and u_2 in Ω . ■

We now have all of the elements needed to prove Theorem 2.

Proof of Theorem 2. We assume that $S \in \Theta$. This implies (cf. proof of Theorem 1) that $\nabla u_{S,L} = \langle L, C \rangle \cdot [a, b]$, where $C : \Omega \rightarrow \mathbb{R}_*^4$ and where $[a, b] : \Omega \rightarrow \mathbb{R}^2$ are $C^0(\Omega)$ mappings. This yields $\forall (L_1, L_2) \in \mathcal{L} \times \mathcal{L}, \forall x \in \Omega, \nabla u_{S,L_1}(x) \Psi \nabla u_{S,L_2}(x)$.

Let $\Omega^+ = \{x \in \Omega, [a, b](x) \neq 0\}$. This set is open as $a : \Omega \rightarrow \mathbb{R}$ and $b : \Omega \rightarrow \mathbb{R}$ are $C^0(\Omega)$. Let

$$(B.1) \quad \omega_L = \text{int}(\{x \in \Omega^+, \nabla u_{S,L}(x) = 0\}).$$

This set is also characterized by

$$(B.2) \quad \omega_L = \text{int}(\{x \in \Omega^+, C(x) \in L^\perp\}).$$

From Lemma 1, we get that for almost every $(L_1, L_2) \in \mathcal{L} \times \mathcal{L}$,

$$\omega_{L_1} = \omega_{L_2} = \emptyset.$$

Next, note that

$$\text{int}(\{x \in \Omega, \nabla u_1(x) = 0\}) = \omega_{L_1} \cup (\Omega/\Omega^+),$$

and thus for almost every $(L_1, L_2) \in \mathcal{L} \times \mathcal{L}$,

$$\text{int}(\{x \in \Omega, \nabla u_1(x) = 0\}) = \text{int}(\{x \in \Omega, \nabla u_2(x) = 0\}).$$

It suffices to use Lemma 3 to conclude that for almost every $(L_1, L_2) \in \mathcal{L} \times \mathcal{L}$, u_{S,L_1} and u_{S,L_2} have the same level lines. ■

Appendix C. Other proofs.

Proof of Corollary 1. This is a direct consequence of Theorem 1 and of the fact that two C^1 functions u_1 and u_2 have the same level lines only if $\forall x \in \Omega, \nabla u_1(x) \Psi \nabla u_2(x)$. ■

Let us rephrase Proposition 1 more precisely. Let ω be a subset of Ω , and let $\mathbf{x} \in \Omega$. We define the following notation:

- $\kappa(\mathbf{x}, L)$ is the level line of $u_{S,L}$ such that $x = p(\mathbf{x}) \in \kappa(\mathbf{x}, L)$.
- $\kappa_\omega(\mathbf{x}, L)$ is the level line of $u_{S,L}|_\omega$ such that $x \in \kappa_\omega(\mathbf{x}, L)$.

Proposition 2. Let $(\mathbf{x}_i, \mathbf{x}_j) \in \omega_i \times \omega_j$, where $(i, j) \in I^2$ and $i \neq j$, such that

- there exists $y \in \bar{\kappa}_{\omega_i}(\mathbf{x}_i, L) \cap \bar{\kappa}_{\omega_j}(\mathbf{x}_j, L)$;
- for almost every L' (w.r.t. the Lebesgue measure),

$$\begin{cases} \bar{\kappa}_{\omega_i}(\mathbf{x}_i, L') = \bar{\kappa}_{\omega_i}(\mathbf{x}_i, L), \\ \bar{\kappa}_{\omega_j}(\mathbf{x}_j, L') = \bar{\kappa}_{\omega_j}(\mathbf{x}_j, L). \end{cases}$$

Then

- either we have

$$\lim_{\substack{\mathbf{x} \rightarrow \mathbf{y} \\ \mathbf{x} \in \omega_i}} (N, \alpha)(\mathbf{x}) \neq \lim_{\substack{\mathbf{x} \rightarrow \mathbf{y} \\ \mathbf{x} \in \omega_j}} (N, \alpha)(\mathbf{x}),$$

and for almost every L (w.r.t. the Lebesgue measure), $u_{S,L}(x_i) \neq u_{S,L}(x_j)$,

- or we have

$$\lim_{\substack{\mathbf{x} \rightarrow \mathbf{y} \\ \mathbf{x} \in \omega_i}} (N, \alpha)(\mathbf{x}) = \lim_{\substack{\mathbf{x} \rightarrow \mathbf{y} \\ \mathbf{x} \in \omega_j}} (N, \alpha)(\mathbf{x}),$$

and for almost every L (w.r.t. the Lebesgue measure), $u_{S,L}(x_i) = u_{S,L}(x_j)$.

Proof of Proposition 2. Let $z \in \bar{\kappa}_{\omega_i}(\mathbf{x}_i, L) \cap \bar{\kappa}_{\omega_j}(\mathbf{x}_j, L)$ and $\mathbf{z} = p^{-1}(z)$. We have

$$\forall x \in \kappa_{\omega_i}(\mathbf{x}_i, L), \quad u(x_i) = u(x),$$

and in particular,

$$\begin{aligned} u(x_i) &= \lim_{\substack{\mathbf{x} \rightarrow \mathbf{z} \\ \mathbf{x} \in \omega_i}} u(x) \\ &= \lim_{\substack{\mathbf{x} \rightarrow \mathbf{z} \\ \mathbf{x} \in \omega_i}} ((\langle l, N \rangle + \gamma) \alpha)(\mathbf{x}). \end{aligned}$$

$z \in \bar{\kappa}_{\omega_i}(\mathbf{x}_i, L) \cap \bar{\kappa}_{\omega_j}(\mathbf{x}_j, L)$. Thus, $z \in \bar{\omega}_i \cap \bar{\omega}_j$. As p is a diffeomorphism, $\mathbf{z} \in \bar{\omega}_i \cap \bar{\omega}_j$ (the images by p^{-1} of ω_i and ω_j) and $\lim_{\substack{\mathbf{x} \rightarrow \mathbf{z} \\ \mathbf{x} \in \omega_i}} \mathbf{x} = \mathbf{z}$. Therefore, according to our former hypotheses we can write

$$(C.1) \quad u(x_i) = \left\langle l, \lim_{\substack{\mathbf{x} \rightarrow \mathbf{z} \\ \mathbf{x} \in \omega_i}} (\alpha N)(\mathbf{x}) \right\rangle + \gamma \lim_{\substack{\mathbf{x} \rightarrow \mathbf{z} \\ \mathbf{x} \in \omega_i}} \alpha(\mathbf{x})$$

$$(C.2) \quad = \left\langle l, \lim_{\substack{\mathbf{x} \rightarrow \mathbf{z} \\ \mathbf{x} \in \omega_i}} (\alpha N)(\mathbf{x}) \right\rangle + \gamma \lim_{\substack{\mathbf{x} \rightarrow \mathbf{z} \\ \mathbf{x} \in \omega_i}} \alpha(\mathbf{x}).$$

Similarly, we have

$$(C.3) \quad u(x_j) = \left\langle l, \lim_{\substack{\mathbf{x} \rightarrow \mathbf{z} \\ \mathbf{x} \in \omega_j}} (\alpha N)(\mathbf{x}) \right\rangle + \gamma \lim_{\substack{\mathbf{x} \rightarrow \mathbf{z} \\ \mathbf{x} \in \omega_j}} \alpha(\mathbf{x}).$$

Then $u(x_i) = u(x_j)$ if and only if

$$(C.4) \quad \underbrace{\left\langle l, \lim_{\substack{\mathbf{x} \rightarrow \mathbf{z} \\ \mathbf{x} \in \omega_i}} (\alpha N)(\mathbf{x}) - \lim_{\substack{\mathbf{x} \rightarrow \mathbf{z} \\ \mathbf{x} \in \omega_j}} (\alpha N)(\mathbf{x}) \right\rangle}_{T_1} + \gamma \left(\lim_{\substack{\mathbf{x} \rightarrow \mathbf{z} \\ \mathbf{x} \in \omega_i}} \alpha(\mathbf{x}) - \lim_{\substack{\mathbf{x} \rightarrow \mathbf{z} \\ \mathbf{x} \in \omega_j}} \alpha(\mathbf{x}) \right) = 0.$$

We now consider two cases:

- If $\lim_{\substack{\mathbf{x} \rightarrow \mathbf{y} \\ \mathbf{x} \in \omega_i}} (N, \alpha)(\mathbf{x}) \neq \lim_{\substack{\mathbf{x} \rightarrow \mathbf{y} \\ \mathbf{x} \in \omega_j}} (N, \alpha)(\mathbf{x})$, then (C.4) is verified if and only if L lies in a particular hyperplane of \mathbb{R}^4 . Such a plane is of zero Lebesgue measure.
- If $\lim_{\substack{\mathbf{x} \rightarrow \mathbf{y} \\ \mathbf{x} \in \omega_i}} (N, \alpha)(\mathbf{x}) = \lim_{\substack{\mathbf{x} \rightarrow \mathbf{y} \\ \mathbf{x} \in \omega_j}} (N, \alpha)(\mathbf{x})$, then we fall back to the smooth case; therefore $u_{S,L}(x_i)$ and $u_{S,L}(x_j)$ form a single level line which is invariant for almost every illumination condition (w.r.t. the Lebesgue measure). ■

Acknowledgments. The authors gratefully acknowledge Omid Amini for his considerable help in the proof of Theorem 2. They also thank the anonymous reviewers for their numerous comments which greatly improved the clarity of the proofs and the entire paper. They thank Alexis Baudour, Xavier Descombes, and Véronique Prinnet for fruitful discussions and support during the elaboration of this paper. They would also like to thank the RSIU team at Liama Laboratory, Beijing, for kindly providing the high resolution QuickBird image pairs of Beijing (Figure 9) and F. Lafarge for providing the building library (Figure 6). The second author would like to thank the French Defense Agency (DGA) for partial funding of his doctorate.

REFERENCES

- [1] C. BALLESTER, E. CUBERO-CASTAN, M. GONZALEZ, AND J. MOREL, *Contrast invariant image intersection*, in Advanced Mathematical Methods in Measurement and Instrumentation, Esculapio, Bologna, Italy, 2000, pp. 41–55.
- [2] M. J. BLACK, D. J. FLEET, AND Y. YACOOB, *Robustly estimating changes in image appearance*, Comput. Vis. Image Underst., 78 (2000), pp. 8–31.
- [3] F. CAO AND P. BOUTHEMY, *A general principled method for image similarity validation*, in Adaptive Multimedia Retrieval: User, Context, and Feedback, Lecture Notes in Comput. Sci. 4398, Springer, Berlin, 2007, pp. 57–70.
- [4] V. CASELLES, B. COLL, AND J. M. MOREL, *Topographic maps and local contrast changes in natural images*, Int. J. Comput. Vision, 33 (1999), pp. 5–27.
- [5] V. CASELLES, B. COLL, AND J. M. MOREL, *Geometry and color in natural images*, J. Math. Imaging Vision, 16 (2002), pp. 89–105.
- [6] V. CASELLES, J. L. LISANI, J. M. MOREL, AND G. SAPIRO, *Shape preserving local histogram modification*, IEEE Trans. Image Process., 8 (1999), pp. 220–230.
- [7] V. CASELLES AND P. MONASSE, *Geometric Description of Images as Topographic Maps*, Lecture Notes in Math. 1984, Springer, Berlin, 2010.
- [8] H. F. CHEN, P. N. BELHUMEUR, AND D. W. JACOBS, *In search of illumination invariants*, in Proceedings of the IEEE Computer Society Conference on Computer Vision and Pattern Recognition, 2000, pp. 1254–1261.
- [9] F. COURTELLE, A. CROUZIL, J.-D. DUROU, AND P. GURDJOS, *Shape from shading for the digitization of curved documents*, Mach. Vision Appl., 18 (2007), pp. 301–316.
- [10] M. DROSKE AND M. RUMPF, *A variational approach to nonrigid morphological image registration*, SIAM J. Appl. Math., 64 (2004), pp. 668–687.
- [11] A. FOURNIER, X. DESCOMBES, AND J. ZERUBIA, *Mixing geometric and radiometric features for change classification*, in Computational Imaging VI, Proceedings of SPIE, Vol. 6814, SPIE, Bellingham, WA, 2008, 681408.
- [12] F. GUICHARD AND J.-M. MOREL, *Image Analysis and P.D.E.s*, IPAM GBM Tutorials, 2001.
- [13] B. K. P. HORN AND M. J. BROOKS, *Shape from Shading*, MIT Press, Cambridge, MA, 1989.
- [14] R. B. IRVIN AND D. M. MCKEOWN, *Method for exploiting the relationship between buildings and their shadows in aerial imagery*, IEEE Trans. Systems Man Cybernet., 19 (1989), pp. 1564–1575.
- [15] K. JANISCH, *Topology*, Springer, Berlin, 1984.
- [16] J. J. KOENDERINK AND A. J. VAN DOORN, *Illuminance critical points on generic smooth surfaces*, J. Opt. Soc. Amer. A, 10 (1993), pp. 844–854.
- [17] J. KYBIC AND M. UNSER, *Fast parametric elastic image registration*, IEEE Trans. Image Process., 12 (2003), pp. 1427–1442.
- [18] F. LAFARGE, X. DESCOMBES, J. ZERUBIA, AND M. PIERROT-DESEILLIGNY, *Building reconstruction from a single DEM*, in Proceedings of the IEEE Computer Society Conference on Computer Vision and Pattern Recognition, 2008, pp. 1–8.
- [19] W. LI, X. LI, Y. WU, AND Z. HU, *A novel framework for urban change detection using VHR satellite images*, in Proceedings of the 18th International Conference on Pattern Recognition, IEEE Computer Society, Washington, DC, 2006, pp. 312–315.

- [20] R. LILLESTRAND, *Techniques for change detection*, IEEE Trans. Comput., 21 (1972), pp. 654–659.
- [21] C. LIN AND R. NEVATIA, *Building detection and description from a single intensity image*, Comput. Vis. Image Underst., 72 (1998), pp. 101–121.
- [22] J. L. LISANI AND J. M. MOREL, *Detection of major changes in satellite images*, in Proceedings of the IEEE International Conference on Image Processing, 2003, pp. 941–944.
- [23] D. S. LIU, P. GONG, M. KELLY, AND Q. GUO, *Automatic registration of airborne images with complex local distortion*, Photogram. Eng. Remote Sens., 72 (2006), pp. 1049–1059.
- [24] D. LU, P. MAUSEL, E. BRONDIACUTEZIO, AND E. MORAN, *Change detection techniques*, Int. J. Remote Sensing, 25 (2004), pp. 2365–2407.
- [25] D. MARR, *Vision: A Computational Investigation into the Human Representation and Processing of Visual Information*, W. H. Freeman, New York, 1982.
- [26] L. MOISAN, *Modeling and Image Processing*, lecture notes, École normale supérieure de Cachan, Cachan, France, 2005; available online from http://www.math-info.univ-paris5.fr/~moisan/mva/download.php?file=mva_moisan.pdf.
- [27] P. MONASSE, *Contrast invariant registration of images*, in Proceedings of the IEEE International Conference on Acoustics, Speech, and Signal Processing, Vol. 6, 1999, pp. 3221–3224.
- [28] P. MONASSE AND F. GUICHARD, *Fast computation of a contrast-invariant image representation*, IEEE Trans. Image Process., 9 (2000), pp. 860–872.
- [29] J. MUNDY AND A. ZISSERMAN, *Geometric Invariance in Computer Vision*, MIT Press, Cambridge, MA, 1992.
- [30] B. T. PHONG, *Illumination for computer generated pictures*, Comm. ACM, 18 (1975), pp. 311–317.
- [31] R. J. RADKE, S. ANDRA, O. AL KOFAHI, AND B. ROYSAM, *Image change detection algorithms: A systematic survey*, IEEE Trans. Image Process., 14 (2005), pp. 294–307.
- [32] L. RUDIN, S. OSHER, AND E. FATEMI, *Nonlinear total variation based noise removal*, Phys. D, 60 (1992), pp. 259–268.
- [33] M. SPIVAK, *A Comprehensive Introduction to Differential Geometry*, Vol. 3, Publish or Perish, Houston, 1999.
- [34] C. L. TAN, L. ZHANG, Z. ZHANG, AND T. XIA, *Restoring warped document images through 3D shape modeling*, IEEE Trans. Pattern Anal. Mach. Intell., 28 (2006), pp. 195–208.
- [35] F. TANG AND V. PRINET, *Computing invariants for structural change detection in urban areas*, in Proceedings of the Urban Remote Sensing Joint Event, Paris, 2007, pp. 1–6.
- [36] J. THEILER AND S. PERKINS, *Resampling approach for anomalous change detection*, in Algorithms and Technologies for Multispectral, Hyperspectral, and Ultraspectral Imagery XIII, Proceedings of SPIE, Vol. 6565, SPIE, Bellingham, WA, 2007, 65651U.
- [37] T. A. D. TOTH AND V. METZLER, *Illumination-invariant change detection*, in Proceedings of the 4th IEEE Southwest Symposium on Image Analysis and Interpretation, 2000, pp. 654–659.
- [38] T. WADA, H. UKIDA, AND T. MATSUYAMA, *Shape from shading with interreflections under a proximal light source: Distortion-free copying of an unfolded book*, Int. J. Comput. Vision, 24 (1997), pp. 125–135.
- [39] S. WATANABE, K. MIYAJIMA, AND N. MUKAWA, *Detecting changes of buildings from aerial images using shadow and shading model*, in Proceedings of the Fourteenth International Conference on Pattern Recognition, IEEE Computer Society, Washington, DC, 1998, pp. 1408–1412.
- [40] P. WEISS, L. BLANC-FÉRAUD, AND G. AUBERT, *Efficient schemes for total variation minimization under constraints in image processing*, SIAM J. Sci. Comput., 31 (2009), pp. 2047–2080.
- [41] R. WIEMKER, *An iterative spectral-spatial Bayesian labeling approach for unsupervised robust change detection on remotely sensed multispectral imagery*, in Proceedings of the 7th International Conference on Computer Analysis of Images and Patterns, Springer, London, 1997, pp. 263–270.